ChemComm

Accepted Manuscript

This article can be cited before page numbers have been issued, to do this please use: C. Xiong, W. Liang, H. Wang, Y. Zheng, Y. Zhuo, Y. Chai and R. Yuan, *Chem. Commun.*, 2016, DOI: 10.1039/C6CC01078D.

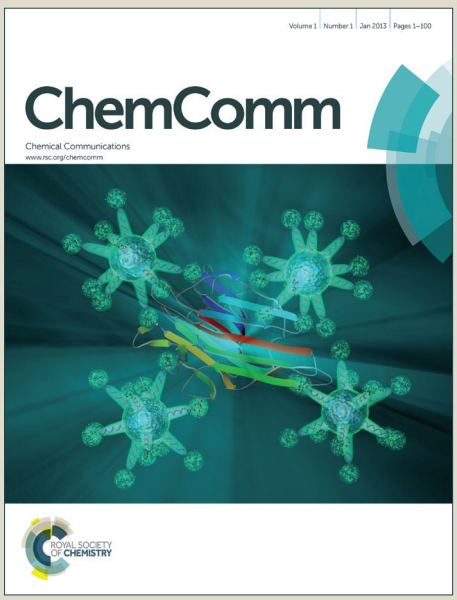

ROYAL SOCIETY OF CHEMISTRY

www.rsc.org/chemcomm

Dynamic Article Links►
View Article Online
DOI: 10.1039/C6CC01078D

Cite this: DOI: 10.1039/c0xx00000x

www.rsc.org/xxxxxx

ARTICLE TYPE

In Situ Electro-polymerization of Nitrogen doped Carbon Dots and Its Application in Electrochemiluminescence Biosensor for the Detection of Intracellular Lead Ion

Chengyi Xiong,[1] Wenbin Liang,[1,2] Haijun Wang,[1] Yingning Zheng,[1] Ying Zhuo,[1] Yaqin Chai*,[1] and Ruo Yuan*,[1]

Received (in XXX, XXX) Xth XXXXXXXXX 20XX, Accepted Xth XXXXXXXXX 20XX
DOI: 10.1039/b000000x

Here, a novel sensitive electrochemiluminescence (ECL) biosensor using N doped carbon dots (N-CDs) in situ electro-polymerized on glass carbon electrode (GCE) as luminophor and Pd-Au hexoctahedrons (Pd@Au HOHs) as enhancer was developed for the detection of intracellular lead ion (Pb^{2+}).

Lead, as a common environmental pollutant, has attracted people's attention since its toxicity was widely reported.[1-5] According to previous literatures, lead ion (Pb^{2+}) even in a small amount can cause serious organ damage to human, especially in children, by irreversible brain damage, mental neurons, lung and some other body tissue.[6, 7] In view of this, several analytical methods have been developed for the detection of Pb^{2+} in human body, including atomic absorption spectrometry,[8] electrochemistry,[9] fluorescence,[10, 11] inductively coupled plasma mass spectrometry (ICP-MS)[12] and so on. However, most of these methods suffer from long analysis time or bulky instrument. And much attention has been paid to the detection of extracellular Pb^{2+}, such as blood lead. However, the concentration of extracellular Pb^{2+} cannot reflect the real amount of Pb^{2+} that causes DNA damage and chromosome aberrations in cells. And the mechanisms of Pb^{2+} toxicity remain an open question for research. In view of these, the accurate detection of the intracellular Pb^{2+} may have more positive significance for clinical diagnosis and help people to understand the lesions mechanism of Pb^{2+}.

Electrochemiluminescence (ECL) technology has been developed rapidly due to its low background, high sensitivity, simple format and may become a powerful tool for the detection of intracellular Pb^{2+}.[13-15] In addition, to broaden the application of ECL in biological analysis, several kinds of novel luminescent materials with excellent biocompatibility have been introduced into ECL system, such as fluorescent dyes,[16] noble-metal nanoclusters,[17, 18] iridium complex[19] and carbon dots (CDs).[20-22] Among these luminescent materials, CDs are easy to be prepared, size-controllable and have superior biological compatibility. Whereas, the luminescence efficiency of traditional CDs is very low. Moreover, the water solubility of CDs makes them difficult to be immobilized on electrode, which further limits their application in ECL system. Therefore, the key point to use CDs as signal probe effectively in ECL system may lie on enhancing the ECL intensity of CDs and immobilizing CDs well. On these accounts, some previous literatures have reported that nitrogen (N) doped CDs have higher luminescence efficiency than traditional CDs.[23-27] And o-phenylenediamine (OPD), a well-known precursor of CDs, which has carbon and nitrogen in its molecule, can be utilized as carbon source and nitrogen source to synthesize N doped CDs (N-CDs).[28, 29] To further enhance the ECL signal of N-CDs, core-shell Pd-Au hexoctahedrons (Pd@Au HOHs) with special catalyst activity for ECL reaction are introduced into the fabrication of ECL biosensor based on N-CDs.[30, 31]

Here, an ECL biosensor using N-CDs in situ electro-polymerized on glass carbon electrode (GCE) as luminophor and Pd-Au hexoctahedron (Pd@Au HOHs) as enhancer was developed for the detection of intracellular Pb^{2+}. As illustrated in Scheme 1, OPD was in situ electro-polymerized on the glass carbon electrode to form N-CDs. Due to the presence of amino groups on N-CDs, Ag nanoparticles (AgNPs) were immobilized on the electrode. In turn, amino-modified capture DNA (T_1) was immobilized on the AgNPs through Ag-N bond. Afterward, the complementary DNA (T_2) and ssDNA1 (S_1) labeled Pd@Au HOHs (Pd@Au HOHs-T_2-S_1) were modified on the electrode through the chain hybridization between T_1 and T_2. Simultaneously, ssDNA2 (S_2) labeled Pd@Au HOHs (Pd@Au HOHs-S_2) were introduced by the hybridization between S_1 and S_2, with the formation of Pd@Au HOHs-DNA dendrimers on the electrode. Owing to highly catalyst activity of Pd@Au HOHs, the ECL reaction of N-CDs was promoted and the signal of N-CDs was significantly enhanced. Finally, intracellular Pb^{2+} was used to couple with numerous repeated DNA sequences of S_1 and S_2 to form Pb^{2+}-stabilized G-quadruplex (G4) structure. With the forming of Pb^{2+}-stabilized G4 structure, the ECL intensity of N-CDs was quenched by Pb^{2+}. Therefore, the ECL biosensor based on N-CDs was successfully fabricated for the detection of intracellular Pb^{2+}. In addition, Pd@Au HOHs-DNA dendrimers not only greatly enhanced the ECL signal of N-CDs, but also realized the effectively capture of Pb^{2+}, which was beneficial to improve the sensitivity in a signal-off biosensor for detection of intracellular Pb^{2+}. Therefore, this work provided a novel and effective detection strategy for intracellular Pb^{2+}.

View Article Online
DOI: 10.1039/C6CC01078D

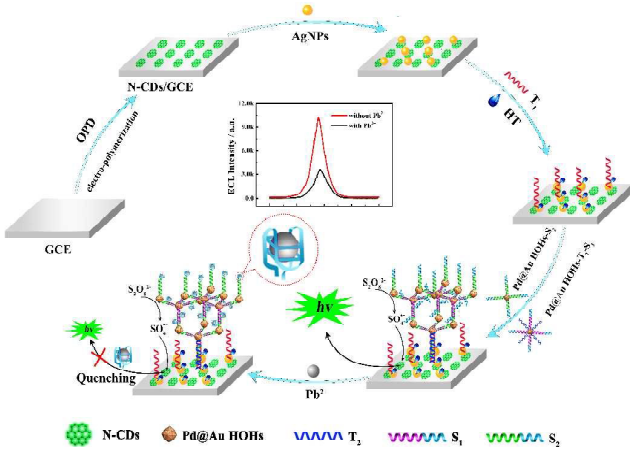

Scheme 1 The fabrication and reaction mechanism of the proposed ECL biosensor.

The possible ECL mechanism of N-CDs was presented in Fig. 1. Firstly, N-CDs got electrons to form N-CDs$^{\bullet-}$. (Reaction ①) With the catalysis of Pd@Au HOHs, $SO_4^{\bullet-}$ was generated more quickly by the oxidation reaction of $S_2O_8^{2-}$, making great contribution to next ECL reactions and leading to the increase of ECL signal. (Reaction ②) After that, the N-CDs$^{\bullet-}$ reacted with $SO_4^{\bullet-}$ to generate N-CDs*. (Reaction ③) Finally, the light emission was produced when the N-CDs* transferred to N-CDs. (Reaction ④). When Pb^{2+}-stabilized G4 structure was forming on the electrode, the ECL intensity of N-CDs was quenched by Pb^{2+} (Reaction ⑤).

$$\text{N-CDs} + n e^- \longrightarrow n\text{N-CDs}^{\bullet-} \quad ①$$

$$S_2O_8^{2-} + e^- \xrightarrow{\text{Pd@Au HOHs}} SO_4^{2-} + SO_4^{\bullet-} \quad ②$$

$$\text{N-CDs}^{\bullet-} + SO_4^{\bullet-} \longrightarrow \text{N-CDs}^* + SO_4^{2-} \quad ③$$

$$\text{N-CDs}^* \longrightarrow \text{N-CDs} + h\nu \quad ④$$

$$\text{N-CDs}^* \xrightarrow{Pb^{2+}} \text{N-CDs} + h\nu \quad ⑤$$

Fig. 1 The possible ECL mechanism of N-CDs.

The morphologies of different nanomaterials were characterized by SEM and TEM. As shown in Fig. S1A (See ESI), AgNPs were well separated spherical particles with a diameter of 10 nm. The images in Fig. S1B presented that the N-CDs were monodisperse nanoparticles with a diameter of 5 nm. The images in Fig. S1C and Fig. S1D revealed that the Pd@Au HOHs possessed polyhedral shape with a diameter of 90 nm. To futhur characterize the synthesis of Pd@Au HOHs, X-ray photoelectron spectroscopy (XPS) was utilized for the elemental analysis of Pd@Au HOHs. As anticipated, the characteristic peaks for Pd3d and Au4f could be observed in Fig. S1E. The peak at 335.0 eV was represented the XPS signature of Pd3d resulting the presence of Pd seeds. The peak at 87.7 eV was the XPS signature of Au4f indicating the existence of metallic Au^0. These proof indicated the successful synthesis of Pd@Au HOHs.

In addition, mostly traditional gold nanomaterials had strong quenching effect for luminescent carbon dots due to the energy transfer between them.[32-34] However, the Pd@Au HOHs prepared in this work greatly enhanced the ECL intensity of N-CDs. The possible reason might be that the UV-vis absorbance spectrum of Pd@Au HOHs was not match with the ECL spectrum of N-CDs well. As shown in Fig. S1F, the UV-vis absorbance spectrum of Pd@Au HOHs had a singular absorbance peak at 649 nm. However, the ECL emission peak of N-CDs was at 556nm in Fig. S1G, which was far from the major absorbance peak of Pd@Au HOHs. Thus, there might be no obvious strong energy transfer between Pd@Au HOHs and N-CDs, which could quench the ECL of N-CDs significantly. Furthermore, Pd@Au HOHs could catalyze the oxidation reaction of $S_2O_8^{2-}$ to generate $SO_4^{\bullet-}$, which contributed to the ECL signal of N-CDs.

The fabrication process of the proposed biosensor was characterized by cyclic voltammetry (CV), which was performed for different modified electrodes in 5 mM $[Fe(CN)_6]^{3-/4-}$ (acting as a redox probe) to evaluate interfacial changes in the construction of the ECL biosensor. As it was presented in Fig. S2A (See ESI), the bare GCE showed a pair of well-defined redox peaks of $[Fe(CN)_6]^{3-/4-}$ (curve a). When N-CDs were synthesized on the surface of electrode, the redox peak current decreased (curve b). The possible interpretation was that N-CDs were semiconductor materials and might hinder electron transport. Due to the superior conductivity of AgNPs, the redox peak current increased significantly after AgNPs were modified on the GCE (curve c). While T_1 (curve d) and HT (curve e) was modified on the electrode, clear decreasing of redox peak currents were observed accordingly. The reason was that T_1 and HT could retard the electron transfer. Subsequently, redox peak current increased again when Pd@HOHs-DNA dendrimers were modified on the electrode, owing to the excellent conductivity of Pd@Au HOHs (curve f).

For further illustrating the fabrication process of the ECL biosensor, the proposed biosensor was characterized by ECL in 3 mL of PBS (pH 7.4, 0.1 M). As shown in Fig. S2B, firstly, there was a weak ECL signal observed when N-CDs were synthesized on the GCE (curve a). Then, the ECL response increased after AgNPs were modified on the electrode (curve b). The possible reason might be that AgNPs could increase the rate of electron transport obviously. After the T_1 (curve c) and HT (curve d) were modified on GCE, the ECL signals decreased respectively. The reason might be that both T_1 and HT could retard the electron transfer. Finally, the ECL response increased significantly when Pd@Au HOHs-DNA dendrimers were immobilized on the GCE (curve e). The potential reason was that Pd@Au HOHs could not only promote transmission of electron, but also have strong enhancement for ECL of CDs. All of these observations proved that the proposed ECL biosensor was fabricated successfully.

The dynamic linear range of the proposed ECL biosensor was evaluated by incubating cell lysis buffer containing different concentrations of Pb^{2+} (the concentrations of Pb^{2+} in cell lysis buffer was calibrated by ICP-MS). Fig. 2A showed the ECL response measured at various cell lysis buffer containing different concentration of Pb^{2+}. The ECL signal was decreased with increasing the concentration of intracellular Pb^{2+}. The calibration plot displayed a good linear relationship between ECL intensity and the logarithm of the concentration of intracellular Pb^{2+} in a range of 1.0 ng mL^{-1} to 1375.0 ng mL^{-1}. The detection limit was 0.33 ng mL^{-1}. The regression equation was I = -2002.6 lgc_{Pb2+} + 9516.0 with a correlation coefficient of R = 0.9932. The results displayed that the proposed biosensor could be an appropriate tool for the detection of intracellular Pb^{2+}.

The ECL stability of the proposed biosensor was monitored in this work. As it was presented in Fig. 2B, the ECL intensity increased with decreasing the concentration of intracellular Pb^{2+} and a relatively stable ECL curve at every concentration of intracellular Pb^{2+} could be received. These indicated that the proposed ECL biosensor had good stability for the detection of

View Article Online
DOI: 10.1039/C6CC01078D

intracellular Pb^{2+}. The satisfied stability might be owing to the stable immobilization of N-CDs.

The relative standard deviations (RSDs) of the ECL response of intra- and inter-assays were applied to assess the reproducibility of the proposed ECL biosensor. To get the intra-assays of the biosensor, four electrodes were independently prepared under the same conditions to detect intracellular Pb^{2+} (130.0 ng mL^{-1}) at the same time. To get the inter-assays of the proposed biosensor, an electrode was prepared under the same conditions to detect intracellular Pb^{2+} of 130.0 ng mL^{-1} three times. The RSDs of intra- and inter-assays (130.0 ng mL^{-1}) were not more than 5%, which demonstrated that the proposed ECL biosensor had acceptable reproducibility.

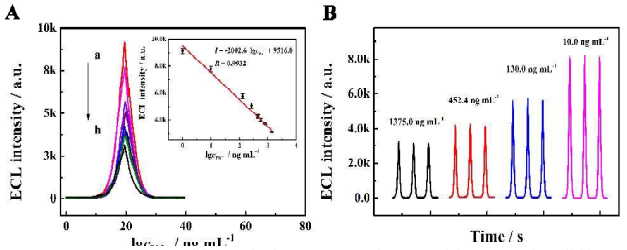

Fig. 2 (A) ECL profiles of the proposed ECL biosenos in different concentrations of Pb^{2+}: a) 1375.0, b) 790.5, c) 559.4, d) 452.4, e) 265.0, f) 129.7, g) 10.0, and h) 1.0 ng mL^{-1}. The inset shows the logarithmic calibration curve for Pb^{2+} in 0.1 M PBS (pH 7.4). (B) The ECL stability of proposed ECL biosenor to various concentrations of intracellular Pb^{2+}.

In summary, a sensitive ECL biosensor using in situ electropolymerized N-CDs as lumophor and Pd@Au HOHs as enhancer was developed for the detection of intracellular Pb^{2+}. The proposed biosensor performed good sensitivity and accuracy for the detection of intracellular Pb^{2+}. Furthermore, the proposed ECL biosensor presented a novel way to apply N-CDs in ECL system in which the ECL signal of N-CDs could be effectively enhanced by Pd@Au HOHs. This method hold great potential for further application in the research of intracellular heavy metal ion related biological process.

This work was financially supported by the NNSF of China (51473136, 21275119, 21575116 and 81301518) and the Fundamental Research Funds for the Central Universities (XDJK2014C138 and XDJK2015A002).

Notes and references

[1]*Key Laboratory of Luminescent and Real-Time Analytical Chemistry (Southwest University), Ministry of Education, College of Chemistry and Chemical Engineering, Southwest University, Chongqing 400715, PR China*

[2]*Department of Clinical Biochemistry, Laboratory Sciences, Third Military Medical University, 30 Gaotanyan Street, Shapingba District, Chongqing 400038, China*
PR China

Fax: +86-23-68253172; Tel: +86-023-68252277; E-mail: yqchai@swu.edu.cn (YQ. Chai), yuanruo@swu.edu.cn (R. Yuan).

† Electronic Supplementary Information (ESI) available: [Experimental; reagents and material; apparatus; synthesis of Ag nanoparticles; preparation of convex Pd@Au HOHs and the preparation of Pd@Au HOHs-T_2-S_1 and Pd@Au HOHs-S_2 bioconjugates; cell culture and cell lysis buffer preparation; fabrication of the ECL biosensor; measurement procedure; Fig.S1; Fig. S2. See DOI:10.1039/b000000x/

1 Y. L. Shang, Y. Q. Zhang, P. Li, J. Lai, X. Y. Kong, W. D. Liu, K. Xiao, G. H. Xie, Y. Tian, L. P. Wen and L. Jiang, *Chem. Commun.*, 2015, **51,** 5979-5981.

2 G. Pelossof, R. Tel-Vered, and I. Willner, *Anal. Chem.*, 2012, **84,** 3703-3709.

3 Z. Q. Yuan, M. H. Peng, Y. He and E. S. Yeung, *Chem. Commun.*, 2011, **47,** 11981-11983.

4 Y. X. Qi, M. Zhang, Q. Q. Fu, R. Liu and G. Y. Shi, *Chem. Commun.*, 2013, **49,** 10599-10601.

5 S. DasGupta, S. A. Shelke, N. S. Li and J. A. Piccirilli, *Chem. Commun.*, 2015, **51,** 9034-9037.

6 N. Tassali, N. Kotera, C. Boutin, E. Leonce, Y. Boulard, B. Rousseau, E. Dubost, F. Taran, T. Brotin, J. P. Dutaste and P. Berthault, *Anal. Chem.*, 2014, **86,** 1783-1788.

7 K. A. Morales, M. Lasagna, A. V. Gribenko, Y. Yoon, G. D. Reinhart, J. C. Lee, W. Cho, P. W. Li, and T. I. Igumenova, *J. Am. Chem. Soc.*, 2011, **133,** 10599-10611.

8 A. Islam, H. Ahmad, N. Zaidi and S. Kumar, *ACS Appl. Mater. Interfaces* 2014, **6,** 13257-13265.

9 Y. Xiao, A. A. Rowe, and K. W. Plaxco, *J. Am. Chem. Soc.*, 2007, **129,** 262-263.

10 T. Li, S. J. Dong, and E. K. Wang, *J. Am. Chem. Soc.*, 2010, **132,** 13156-13157.

11 L. J. Xu, X. Q. Shen, S. N. Hong, J. Wang, Y. Y. Zhang, H. Y. Wang, J. Y. Zhang and R. J. Pei, *Chem. Commun.*, 2015, **51,** 8165-8168.

12 L. Moens, T. D. Smaele and R. Dams, *Anal. Chem.*, 1997, **69,** 1604-1611.

13 Y. M. Lei, W. X. Huang, M. Zhao, Y. Q. Chai, R. Yuan, and Y. Zhuo, *Anal. Chem.*, 2015, **87,** 7787-7794.

14 L. R. Xu, Y. Li, S. Z. Wu, X. H. Liu, and Bin Su, *Angew. Chem. Int. Ed.*, 2012, **51,** 8068-8072.

15 K. N. Swanick, M. Sandroni, Z. F. Ding and E. Z. Colman, *Chem. Eur. J.*, 2015, **21,** 7435-7440.

16 M. Shen, J. R. Lopez, J. Huang, Q. Liu, X. H. Zhu and A. J. Bard, *J. Am. Chem. Soc.*, 2010, **132,** 13453-13461.

17 W. W. Guo, J. P. Yuan and E. K. Wang, *Chem. Commun.*, 2012, **48,** 3076-3078.

18 L. L. Li, H. Y. Liu, Y. Y. Shen, J. R. Zhang and J. J. Zhu, *Anal. Chem.*, 2011, **83,** 661-665.

19 K. N. Swanick, S. Ladouceur, E. Z. Colman and Z. F. Ding, *Angew. Chem. Int. Ed.*, 2012, **51,** 11079-11082.

20 Y. Q. Dong, W. R. Tian, S. Y. Ren, R. P. Dai, Y. W. Chi and G. N. Chen, *ACS Appl. Mater. Interfaces*, 2014, **6,** 1646-1651.

21 Y. Q. Dong, N. N. Zhou, X. M. Lin, J. P. Lin, Y. W. Chi and G. N. Chen, *Chem. Mater.*, 2010, **22,** 5895-5899.

22 J. Hou, L. Wang, P. Zhang, Y. Xu and L. Dan, *Chem. Commun.*, 2015, **51,** 17768-17771.

23 T. Q. Han, T. Yan, Y. Y. Li, W. Cao, X. H. Pang, Q. J. Huang and Q. Wei, *Carbon*, 2015, **91,** 144-152.

24 Y. Q. Dong, H. C. Pang, H. B. Yang, C. X. Guo, J. W. Shao, Y. W. Chi, C. M. Li, and T. Yu, *Angew. Chem. Int. Ed.*, 2013, **52,** 7800-7804.

25 Y. Q. Dong, R. X. Wang, G. L. Li, C. Q. Chen, Y. W. Chi and G. N. Chen, *Anal. Chem.*, 2012, **84,** 6220-6224.

26 A. Gupta, A. Chaudhary, P. Mehta, C. Dwivedi, S. Khan, N. C. Verma and C. K. Nandi, *Chem. Commun.*, 2015, **51,** 10750-10753.

27 Y. F. Kang, Y. W. Fang, Y. H. Li, W. Li and X. B. Yin, *Chem. Commun.*, 2015, **51,** 16956-16959.

28 K. Jiang, S. Sun, L. Zhang, Y. Lu, A. G. Wu, C. Z. Cai and Hengwei Lin, *Angew. Chem. Int. Ed.*, 2015, **54,** 5360-5363.

29 M. Vedamalai, A. P. Periasamy, C. W. Wang, Y. T. Tseng, L. C. Ho, C. C. Shih and H. T. Chan, *Nanoscale*, 2014, **6,** 13119-13125.

30 Y. T. Liu, Q. Q. Zhang, H. J. Wang, Y. L. Yuan, Y. Q. Chai and R. Yuan, *Biosens. Bioelectron.*, 2015, **71,** 164-170.

31 L. Zhang, W. X. Niu, W. Y. Gao, L. M. Qi, J. P. Lai, J. M. Zhao and G. B. Xu, *ACS nano*, 2014, **8,** 5953-5958.

32 Y. P. Shi, Y. Pan, H. Zhang, Z. M. Zhang, M. J. Li, C. Q. Yi and M. S. Yang, *Biosens. Bioelectron.*, 2014, **56,** 39-45.

33 J. Q. Liu, X. X. He, K. M. Wang, D. G. He, Y. H. Wang, Y. F. Mao, H. Shi and L. Wen, *Biosens. Bioelectron.*, 2015, **70,** 54-60.

34 L. L. Wang, J. Zhang, S. Yang, C. C. Wu, C. H. Liu, Y. Xiao, Y. H. Li, Z. H. Qing and R. H. Yang, *ACS Appl. Mater. Interfaces*, 2015, **7,** 19509-19515.